

**Temperature Error Compensation of a Miniature
Semiconductor Pressure Transducer and First Results
of Measurements Taken in a Ducted Propfan Rotor**

**M. Maass
DLR Köln, Germany**

**Temperature Error Compensation of a Miniature
Semiconductor Pressure Transducer and First Results
of Measurements Taken in a Ducted Propfan Rotor**

**M. Maass
DLR Köln, Germany**

Summary

To investigate the unsteady physical flow properties in the outlet of a ducted propfan rotor measurements with a traversed high speed probe and the Laser-2-Focus system have been investigated. In order to measure total pressure rise more precisely a temperature error compensation method and a modification of the single pressure probe have been developed. In combination with the Laser-2-Focus measurements the local isentropic efficiency is calculated for a propfan rotor with low total pressure ratio. This paper discusses the system and the experiences obtained by calibration tests of the single high speed probe and first measurement results are presented.

Introduction

The Institute For Propulsion Technology of the German Aerospace Establishment (DLR) is engaged in programmes to investigate unsteady flows within axial compressors and propfans. Thus measurement techniques are optimized for determining the flow values more accurately in order to avail a data base for code validation too. The unsteady pressure measurements with single high speed probes make possible to have a detailed look into the physics of the turbomachinery flow. With the temperature error compensation method developed in this context transducers are used as absolute pressure sensors. It is well known that using conventional probes the mean values of a fluctuating pressure field in the rotor outlet can not be measured accurately. However, with the digitized signal these values can be also determined more accurately when the pressure ratio decreases. This paper discusses an easily implemented system to provide a miniature high speed pressure probe

used as an absolute pressure probe. The calibration of the probe and a modification of the transducer head is described. Finally first results of unsteady measurements are briefly presented. These have been conducted in a ducted propfan rotor by the 3D-Laser-2-Focus system [3] and the single high speed probe.

1 Temperature Error Compensation System

There are two problems in manufacturing miniature high speed probes: One is to put the Wheatstone bridge elements on the diaphragm at the location of same mechanical stress. The other difficulty is to get the exact semiconductor resistance for each bridge element. However, these are important factors that affect transducer *pressure sensitivity, linearity* and *zero offset*. A measurement error of more than 10% of Full Scale Output (FSO) is obtained with a passive compensation network which is provided by the manufacturer. A more accurate temperature error compensation is evidently needed. One way is to do a temperature error compensation method based on calibration tests as a postprocessing. That means that the digitized raw data are converted into pressure values using the calibration data. Such a method has been presented [1] [2] and it seems to be relatively easy to implement and to use this method for reducing the measurement errors. The method is based on the fact that changes in temperature cause a change in the strain gauge bridge resistance. Such a change of resistance can be easily measured by a change in voltage drop, if the probe is driven by constant current. That means that two voltages have to be measured to calculate pressure and temperature. The unknown temperature of the diaphragm can be eliminated. Fig 1a shows the circuit diagram for a strain gauge bridge and fig 1b shows how it is used in the application. The voltage V_1 is the output which normally is used. The voltage V_2 indicates the second voltage obtained from the resistance of the entire bridge. In fig 1b the ohmic resistances effect a reverse voltage in such a way that the voltage V_2 at different temperatures is around zero. With this system calibration tests have been done with several Kulite XB-21-062-5D transducers.

2 Transducer Calibration

Figure 2a shows the calibration data for the voltage V_1 and fig 2b the data of the voltage V_2 which can be obtained simultaneously by changing the pressure and the temperature in an automatically operated calibration facility. During a calibration test the transducer is put into a big copper block and the heat transfer between the copper block and the transducer is given by heat conduction paste. The temperature of the copper block is measured by a platinum resistance thermometer and it is assumed that the temperature of the copper block is equal to the temperature of the diaphragm. The signal V_1 in fig 2a shows the pressure dependance on temperature, the zero offset and the thermal zero drift. The signal V_2 nearly dependents on temperature. Both signals are non-linear. The temperature measured by V_2 is the temperature of the diaphragm. A direct interpretation

as a temperature of fluid is not correct. Probably the non-linearity increases because the transducer is driven by constant current. But this behaviour will be compensated by this method. In the turbomachinery tests the two voltages output signals are converted into pressure values using this calibration curves.

3 Evaluation of Pressure Values

The two voltages V_1 and V_2 obtained during a calibration test represent a functional dependence on pressure and temperature:

$$V_1 = f(P, T) \quad (1)$$

$$V_2 = f(P, T) \quad (2)$$

These equations can be approximated into polynomials as shown for V_1

$$v_1 = \sum_{i=1}^m \sum_{j=1}^n a_{ij} * P^{i-1} * T^{j-1} \quad (3)$$

$$(4)$$

With the least squares method the $q = m * n$ independent coefficients are determined by solving a system of q equations.

$$Q_1 = \sum_{r=1}^u \sum_{s=1}^w (v_1(P, T) - \hat{v})^2 \quad (5)$$

with

\hat{v} : Measured Values of $V_1(P, T)$

u : Number of calibrated points of P

w : Number of calibrated points of T

The equations are solved by formulating the least squares condition as

$$\frac{\partial Q_1}{\partial a_{11}} = 0, \quad \frac{\partial Q_1}{\partial a_{12}} = 0 \quad \dots \quad \frac{\partial Q_1}{\partial a_{ij}} = 0 \quad \dots \quad \frac{\partial Q_1}{\partial a_{mn}} = 0. \quad (6)$$

These system of equations are then solved by Gaussian Elimination Method. It could also be determined by the matrix method according to Falk scheme.

Polynomials of an order higher than 3 or 4 will not be much more accurate. Polynomials of an order higher than 7 can overshoot and give incorrect results.

The conversion from voltage to pressure data is done by the Newton iteration method. It is evident that non-linearity of the signal also disappears and causes no more measurement error because of the polynomials approximation.

The measurement error with this system decreases to less than 0.1% FSO.

4 Further Considerations of Signal

Important for this compensation method is the question of repeatability of signal behaviour. Experiences show that approximately only the zero offset is drifting over time. The sensitivity and the thermal behaviour can approximately be kept to constant over one week. Due to this behaviour it is only necessary to check the zero-offset at one calibration point. The safest way is to measure the zero offset short before and short after the measurements in the test facility. It is important not to interrupt the power supply. A mean zero offset is calculated and the determination of absolute pressure values is done with the calibration data relative to the zero offset. Further investigations show a repeatability and hysteresis effects approximately within the manufacturer's specification. Figure 3 shows the repeatability of zero offset over temperature rise measured several times within one week. $0.3mV$ represents approximately $1mbar$ for the transducer used. To check the effects of hysteresis the pressure (fig 4a) is driven from zero to full scale and back to zero at different temperatures. Fig 4b shows the same procedure for the temperature at constant pressure. Investigations at different pressure levels show the same behaviour. The hysteresis error is close to $1mbar$ and seems to be a little higher than manufacturer's specification. After first measurements behind the propfan rotor the pressure level has been found to be lower than expected. This is due to the fact that the transducer is mounted with a protection screen as shown in fig 5. Probably an incomplete stagnation causes a decreased pressure level. This could be modified by sticking a tube over the transducer to get a more complete stagnation value. This recesses the transducer front and the total pressure is captured more completely like in a pitot tube. Von Karman Institut carried out that protruding the transducer by $0.5mm$ seems to be a better compromise between reaching the true pressure level without cutting the frequency response [4].

5 Compressor Measurements

With this temperature error compensation system the total pressure is measured in the outlet of a ducted propfan rotor at the 100% design speed. Fig 6 shows the position of the measurement plane behind the rotor. In the same measurement plane local absolute velocity and local swirl angle are measured at the same axial position by the 3D-Laser-2-Focus system. Fig 7 shows a pressure curve for a relative blade height of 87.8%. The wakes are evident to be seen and also an overshoot appears in the pressure rise near the suction side. Further investigations have to explain this overshoot.

With the local absolute velocity, the local swirl angle and the total temperature of the inlet the local total temperature rise is calculated. Fig 8 shows the local total temperature distribution from blade to blade and from hub to tip. The wake region indicated by the dark gray color can be easily recognized. High losses in the wake will increase the total temperature.

Fig 9 shows the local isentropic efficiency which is calculated from the local temperature and the measured local total pressure. Evident are the wakes with low efficiency. The

overall isentropic efficiency calculated by mass averaging is very close to the expected range for a propfan rotor with a mean total pressure ratio of 1.12.

Conclusions

- Unsteady flow measurements in the turbomachinery with high speed probes using the temperature error compensation method are more accurate than the use of averaging probe.
- The briefly presented method offers to be an accurate method for determining the mean isentropic efficiency even for compressors with low pressure ratio.
- The local total pressure distribution, the total temperature ratio and the local efficiency give the chance to look into more detail of the flow phenomena of turbomachines.

References

- [1] Cherrett, M.A., *Temperature Error Compensation Applied to Pressure Measurements Taken in a High-Speed Research Compressor*, Proceeding, 10th Symposium on Measuring Techniques for Transonic and Supersonic Flows in Cascades and Turbomachines, Von Karman Inst., Brussels, Belgium
- [2] Epstein, A.H., *High Frequency Response Measurements in Turbomachinery*, VKI Lecture Series 1985-03, Brussels, 1985
- [3] Schodl, R., Förster, W., *New developments in the laser-2-focus technique for non-intrusive velocity measurements in gasturbine components* J.Phys.III France 2(1992) 613-627
- [4] Späth, C., *Measurements with a High Speed Rotating Kulite Pressure Probe*, VKI, Brussels, 1992

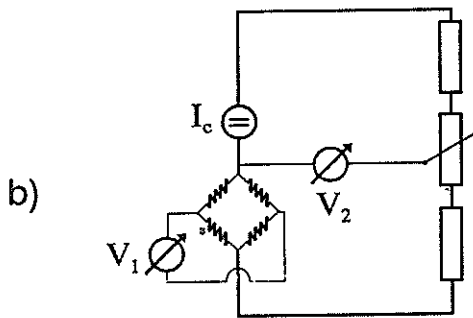
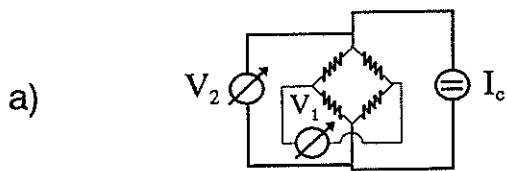


Fig 1 Scheme of "Temperature Error Compensation"

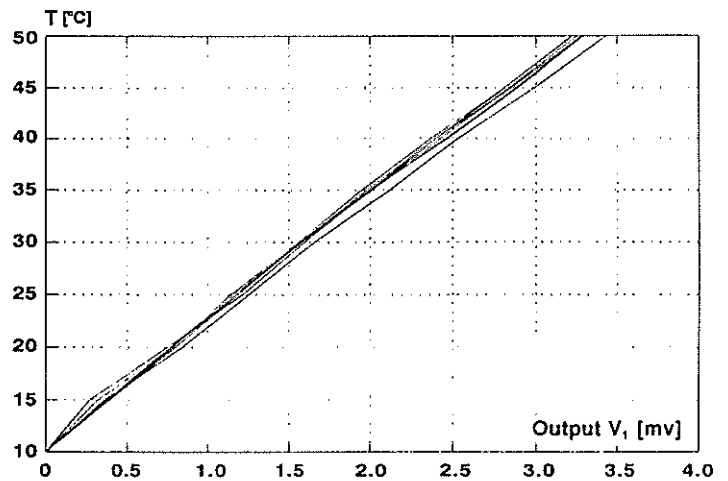


Fig 3 Repeatability of Output V_1 (Zero-Offset, one week)

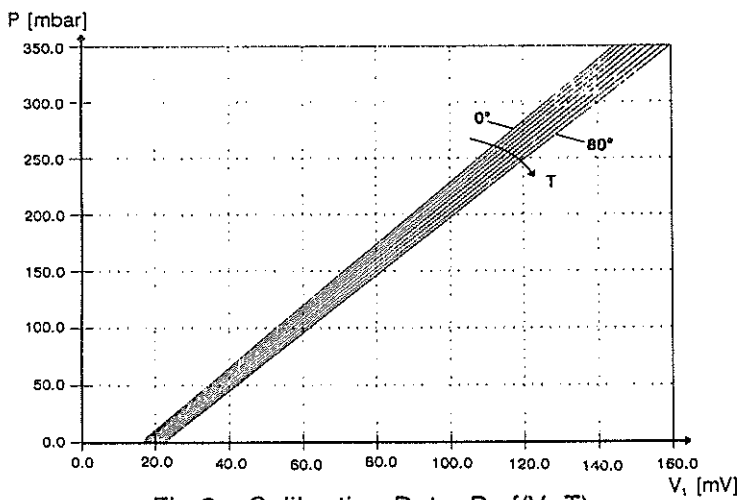


Fig 2a Calibration Data $P=f(V_1, T)$

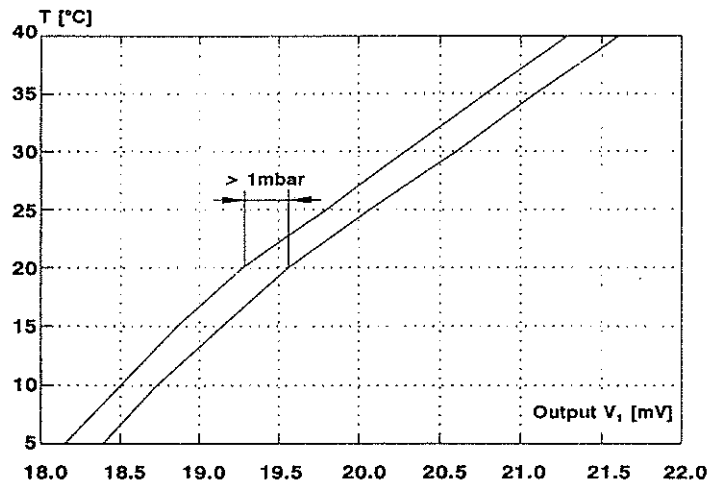


Fig 4a Hysteresis (over Pressure: 0 - 350 - 0 mbar)

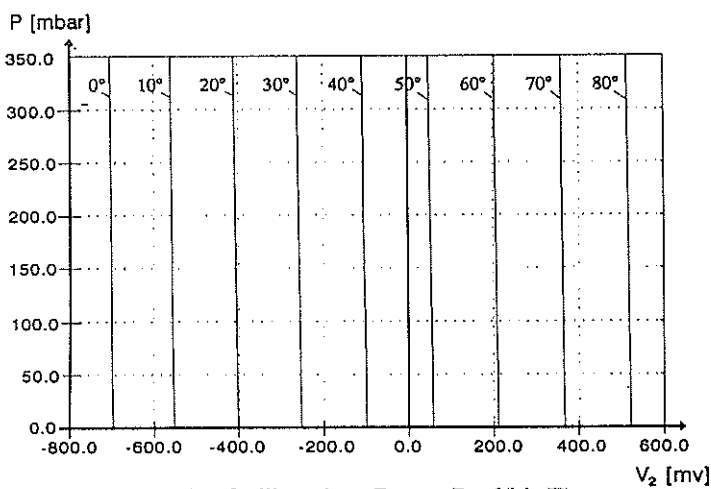


Fig 2b Calibration Data $P=f(V_2, T)$

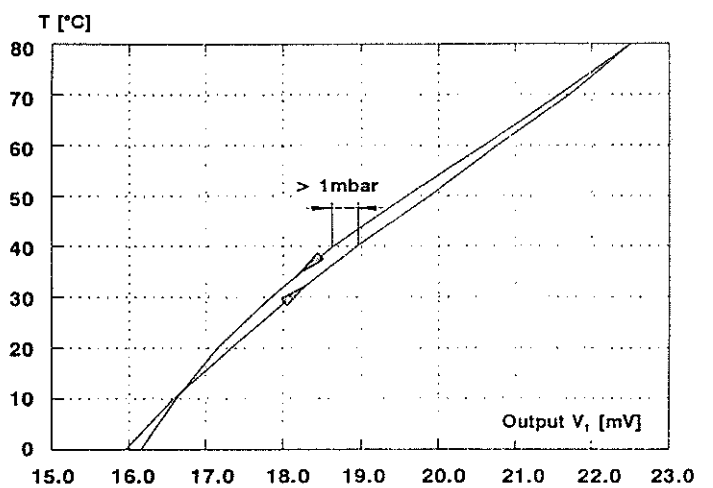


Fig 4b Hysteresis (over Temperature, 0mbar)

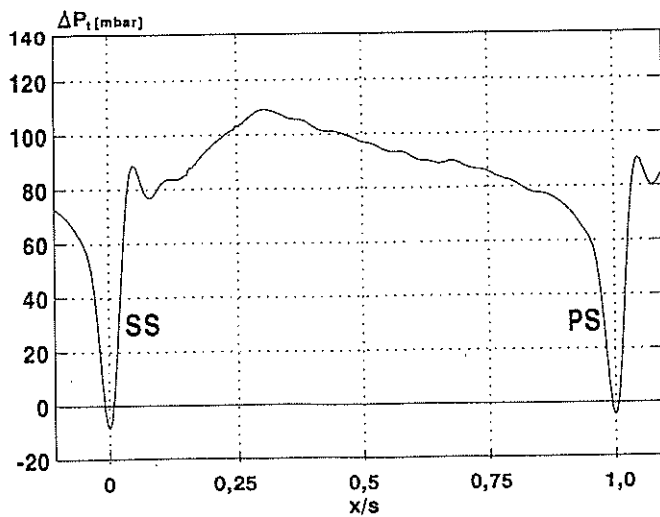
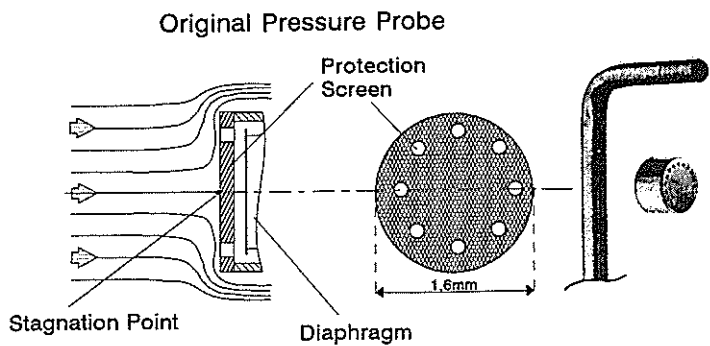


Fig 7 P_t for 87,8% relative blade height
SS: Suction Side, PS: Pressure Side

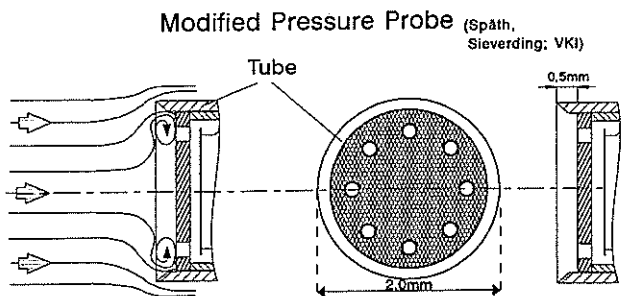


Fig 5 Modified Probe

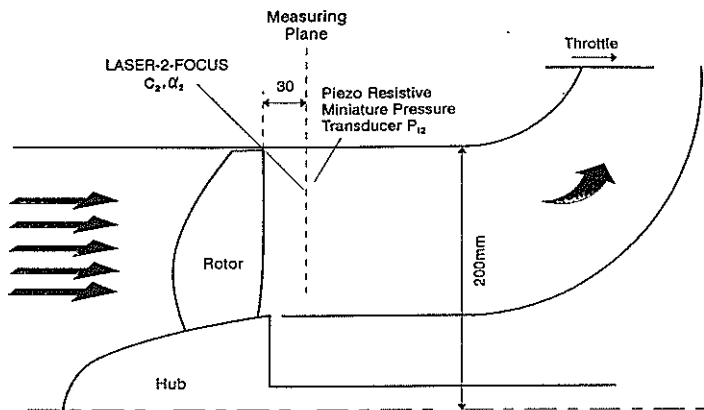


Fig 6 Test Facility CRISP R1

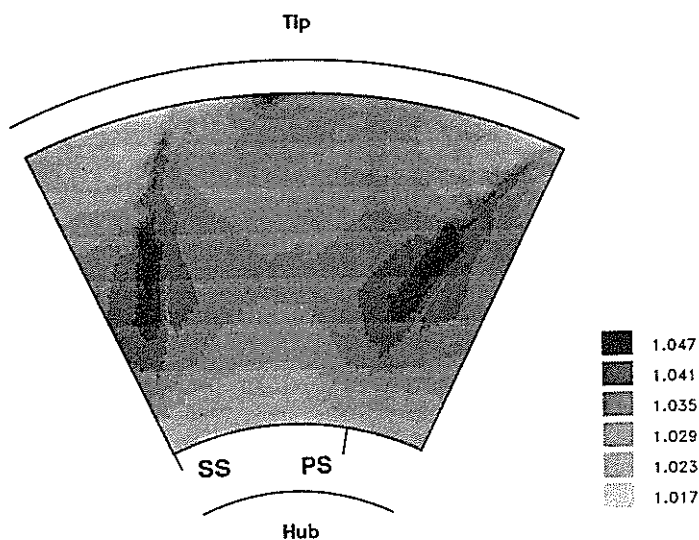


Fig 8 Total Temperature Ratio

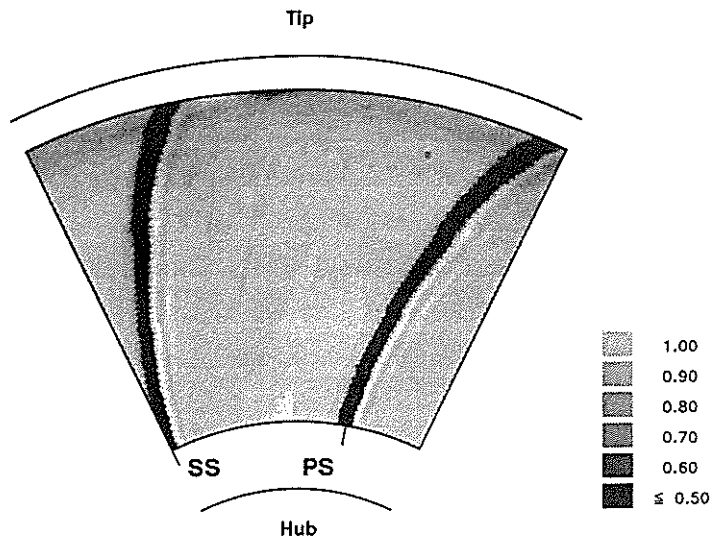


Fig 9 Isentropic Efficiency